Experimental and numerical investigation on aerosols emission in musical practice and efficiency of reduction means

Romain Viala, Milena Creton, Michael Jousserand, Tristan Soubrié, Julien Néchab, Vincent Crenn, Joris Léglise

Experimental and numerical investigation on aerosols emission in musical practice and efficiency of reduction means

Article *in* Journal of Aerosol Science · July 2022

DOI: 10.1016/j.jaerosci.2022.106051

CITATIONS
0

READS
26

7 authors, including:

Romain Viala
Institut Technologique Européen des Metiers de la Musique
32 PUBLICATIONS **89** CITATIONS

SEE PROFILE

Julien Néchab
ANDHEO
1 PUBLICATION **0** CITATIONS

SEE PROFILE

Experimental and numerical investigation on aerosols emission in musical practice and efficiency of reduction means

Romain Viala[a], Milena Creton[b], Michael Jousserand[b], Tristan Soubrié[c], Julien Néchab[c], Vincent Crenn[d], Joris Léglise[d]

[a]*Institut Technologique Européen des Métiers de la Musique, ITEMM, 72000 Le Mans / Laboratoire d'Acoustique de l'Université du Mans — LAUM CNRS 6613 — Le Mans Université, Avenue Olivier Messiaen, 72085 Le Mans Cedex 09, France*
[b]*Buffet Crampon 5 rue Maurice Berteaux, 78711 Mantes-La-Ville, France*
[c]*ANDHEO, Centre ONERA, 29 Avenue de la Division Leclerc, 92322 Châtillon, France*
[d]*ADDAIR, 189 Rue Audemars, 78530 Buc, France*

Abstract

Early in the CoViD-19 pandemic, musical practices, especially singing and playing wind instruments, have been pointed out as having a high risk disease transmission due to aerosol production. However, characterization of these emission sources was not consolidated. This study focuses on the generation of aerosols and potential reduction in the context of playing wind instruments and singing. Aerosol concentration reduction means are evaluated using aerosol measurements in clean room and Computational Fluid Dynamics. Measurements at the bell of a clarinet and in front of singers are performed with or without a protection (bell cover for clarinet and surgical mask for singers). Numerical results on clarinet suggest that most of the supermicron ($\geq 1\ \mu m$) particles are trapped on the walls of the instruments, which act as a filter, depending on toneholes configurations (closed or opened) changing the frequency of sound produced. Experimental results are consistent since almost only submicron particles contribute to the measured number concentration during playing clarinet. First of all, the high inter and intra-individuals variability is highlighted, with high coefficients of variation. This study highlights the impact of fingerings on the generated particles and the efficiency of protections such as bell cover (from 3 to 100 times), depending on the played note and players. Results for singers

show that surgical masks significantly reduce the aerosol concentration (from 8 to 170 times) in front of the mouth. The evolution of aerosol concentration is also correlated with sound intensity.
Keywords: Computational Fluid Dynamics, aerosols measurements, musical practice, woodwind instruments

---

Introduction

During CoViD-19 pandemic, performing arts have been flagged as a risky activity and many practices and representations have been suspended, in order to avoid risks from the public's side as well as from the performers' side. Different categories of transmission risks are defined by the World Health Organization [1]. Transmission risk by fomites can be prevented via disinfection methods, while "Airborne and droplets risk" refers to the inhalation of both "big" or "fine" particles. The latter are generally called "aerosols", though the sizes of emitted particles follow a continuum from gaseous behavior to ballistic items as their size increases [2]. Risk of transmission through aerosols for different diseases has already been established [3, 4] and is considered for the CoViD-19 as a major transmission way. Therefore, it is a preoccupation that should be taken into account for collective musical practice, especially in enclosed areas. Playing wind instruments or singing has been especially pointed out as a risky activity. More precisely, two separate ideas were involved in this assumption : (i) these activities emit large amount of droplets and / or aerosols and (ii) wind instruments also generate air flows that enable these particles to travel up to a certain distance in a room.

Concerning (ii), the propagation of air flows escaping wind instruments has been studied qualitatively using Particle Image Velocimetry [5] or schlieren imaging [6, 7, 8], which showed that air flows can escape through tone holes for woodwinds or leak at the embouchure but mainly exits through the bell. Flow visualizations [7] as well as anemometer measurements [9] indicated that air flows escaping the bell of wind instruments (with exception for air jet instruments

like flute or piccolo) have low velocities and therefore quickly reach the velocity of ambient air flows of the room.

Facing the lack of data in the literature at the beginning of the CoViD-19 crisis, the topic of particle emissions in the musical context has been the object of several works over the years 2020 and 2021. The act of singing has been studied and compared to different kinds of vocalizations and to normal breathing. Studies agreed mainly on the fact that concentrations increase while singing compared with talking at the same sound intensity and that emissions particularly increase with vocal loudness [10, 11, 12], in agreement with the findings of [13] on speech. These studies, especially [10] where 25 performers were taken into account, pointed a very important inter-individual variability.

Up to now, few experimental studies about particle emissions by wind instruments have been published. The studies [14] and [15] did measurements in clean environments using Aerodynamic Particle Sizers (APS) measuring particles between 0.5 and 20 μm. Published work by [14] proposes a classification of wind instruments according to their emission levels, (ranging between 2.10^{-2} and 2 particles per cm^3) for the tuba and the trumpet, respectively. The latter concludes on a distinction between low, intermediate, and high-risk instruments based on a comparison with emissions from breathing and speaking. The labeled high-risk instruments are clarinet, trumpet, oboe, trombone. Measurements on several wind instruments as well as singers and measured concentrations of similar orders of magnitude for both kinds of activities were performed in [15]. To focus on clarinet, the existing data suggests concentrations at the bell of approximately 0.2 particles per cm^3 according to [14], and over one decade higher for [15]. Both studies displayed notable variability among players and had restricted cohorts, therefore highlighting the need for investigations on larger cohorts and with the most repeatable essays as possible. The studies measuring aerosols emitted when singing or playing wind instruments use APS and focus on size ranges starting at 500 nm [16], [15], [14], [10], [11] or 300 nm [12], [17]. Works led on singers show that the emitted particles are mainly submicronic and rarely exceed 3 μm [11] (60 to 70 % particles smaller than 1 μm for loud and normal

singing, respectively), [12] ($>$ 80 % of all particles lower than 1 μm for singing), [18] $>$ 70% of all particles were submicronic for speech, [19] (aerosol mean diameter of 0.75 μm for talking without mask, 72 % of particles being smaller than 1 μm). The study [15] points out a majority of particles smaller than 2.5 μm for both singers and clarinets, the latter emitting more submicronic particles. In a contradictory way, [14] estimated the sizes for a clarinet via a calibration between APS and an imaging system, indicating a size distribution for clarinet following a log normal distribution with a mean size about 2,5 μm.

Though some works exist on the dispersion of emitted particles in the surroundings of the musician using the numeric tool of Computational Fluid Dynamics (CFD) [15], their dispersion inside wind instruments has never been the object of any known publications up to now.

Mitigation methods against airborne transmission involve social distancing as well as prevention of aerosols' accumulation in a room (air renewal, shorter periods of playing), but also relies on limiting particles' emissions at the source. Adequate and well-fitted masks have shown great efficiency also for the specific case of singing [11], [18] and [15]. Using the same principle as masks, so-called "bell covers" have been shown to filter the particles emitted by some wind instruments in [15] and [9].

Indeed, as we could expect, the efficiency of this kind of protection for Brass family instruments where the bell is the only opened hole is clear. But it is more complex in the case of woodwinds instruments such a clarinet where the number of opened and closed tone holes are changing continuously.

Current state of the art faces a lack of knowledge on the inter- and intra-individual variability, as well as on phenomena occurring on the inner part of the instruments, whose study may provide key elements for the comprehension of the discrepancies and variability.

Objectives

The objective of this study is to characterize the aerosol production and propagation of an instrument considered as risky, the B♭ clarinet, a wind instru-

ment from the wood family with a single-reed mouthpiece. For this purpose, Computational Fluid Dynamics and experimental measurements in clean room will be performed to evaluate the impact of tone holes configurations and sound intensity on the particle concentration and size distribution. As a comparison, measurements on singers have been conducted using the same material and conditions. Besides, the impact of bell cover on the reduction of particles emitted by clarinet is addressed and compared to the efficiency of mask wear by singers.

Material and methods

Computations

Computation set-up

Air flows in wind instruments are by nature unsteady. Indeed, the sound results from (i) an exciter as source of vibrations and (ii) a resonator to amplify the vibrations. In the case of clarinet, the exciter is a single reed mounted on a mouthpiece. The resonator is the air column bounded by the instrument tube. There is then a vibration at the source to form sound waves that propagate and are reflected in the tube. However, in the present study, we are interested in simulating air flows in the instrument only as a carrier of particles. As a consequence, a time-averaged air flow, which may not correspond to any instantaneous picture of realistic flows in this framework, is supposed to be a sufficiently good approximation to start investigating how particles emitted by the player are transported inside the instrument and transferred from the instrument to the direct environment. In addition, the instrument is considered fixed in space, which corresponds to the conditions of the measurement campaign, but generally not to realistic playing conditions. Three notes have been simulated on the B♭ clarinet as given hereafter, from the lowest to the highest pitch. Fingerings corresponding to these notes are plotted in appendix (figure 12).
The boundary conditions are set as follows. The mean air flow rate, measured using a Gallus gas meter (see appendix), is specified at the inlet of the tube downstream the mouthpiece. Referenced flow rate is *0.60* m^3/h (*10* l/min). The effect of changes in the flow rate on flow and on particles trajectories has been investigated for note G only, considering also values of *0.45* m^3/h (*7.5* l/min) and *0.75* m^3/h (*12.5* l/min). The air velocity is set uniform over the section. A large volume of air surrounding the isolated instrument is included, at the border of which the environmental pressure with zero-velocity is applied. Thermal effects are neglected. Indeed, the residence time inside instruments is rather short compared to characteristic time for heat transfer. Temperature difference between air escaping from the mouth and the environment may affect fluid

flow distribution close to tone-holes and bell, due to buoyancy effects; however, many other parameters may affect the mixing of inside and outside air, such as ventilation, movements of the musician, hands acting as obstacles to the flow but also heat sources. We have then considered, in a first attempt to model flow inside wind instruments and focusing on particles trajectories, to generally neglect these thermal effects. Similarly, effects of humidity changes or condensation on inner-walls on the flow pattern and wall-shear stress has not been addressed here and is let for future works. Water particles are emitted at the location where air is blown. Diameters of 0.5, 5 and 50 μm (under the assumption of spherical liquid aerosols) are considered and named in the next sections the smallest, medium and largest particles or droplets, respectively. Only one direction of gravity with respect to the instrument is considered, making an angle of 45° with the clarinet body axis. The effect on air flow of the protection at the bell is modeled as an isotropic porous medium. The pressure drop is considered proportional to the velocity to the square. The proportionality factor is calculated using the permeability to air, of 185 $\mathrm{l.m^{-2}.s^{-1}}$, measured for a pressure drop of 100 Pa and delivered by the manufacturer. The effect of the protection on droplets is not modeled. Therefore, the computation does not provide the amount of particles traveling through the bell cover, only the amount reaching the internal face of the protection.

The meshes contain about 0.6 million cells. The basic cell size, far from walls, is 15 mm. It is refined up to 5 times close to walls, reaching 0.5 mm (figure 1). For the considered flow rate, the y^+ ranges from 4 close to the injection plane to 0.5 at the bell inlet. Meshes contain at least 10 cells in the cross-section of the tube or of the tone holes. Details regarding numerical validation and mesh convergence check are provided in appendix.

Solver

Fluid computations are performed using Siemens 2020 FloEFD solver [20] in the framework of *Dassault Systèmes SolidWorks* CAD environment. It solves the Navier-Stokes equations for compressible fluids in the framework of Favre

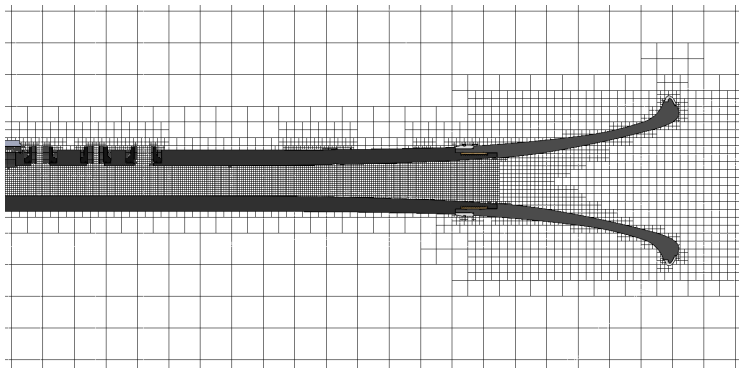

Figure 1: Computational mesh in a median plane of the clarinet through tone holes

averaging. It uses Cartesian meshing technology, with Octree refinement to decrease the size of cells and increase the mesh density where necessary. The turbulence model is of $k - \epsilon$ type. To model the boundary layer at the walls, a technology of so-called "partial/smart cells" is used: in a partial cell, several control volumes are considered, with a minimum of two - one is fluid, the other one is solid - separated by plane faces with respect to the geometry. A specific wall law is applied on those faces to simulate the boundary layer, the so-called *Modified Wall Functions* approach. It uses a Van Driest's profile instead of a logarithmic profile. If the size of the mesh cell near the wall is larger than the boundary layer thickness, the integral boundary layer technology is used. Convergence of steady computations is controlled regarding predefined goals, basically the flow rate on the inlet/outlet, the mean and maximum velocities in the computational domain, and also considering the number of travels of flow particles in the fluid domain. In addition to computing the fluid flow, the software enables to solve the motion of dilute spherical liquid particles (droplets) of constant mass in a steady-state flow field. The particle resistance coefficient (drag coefficient) follows Henderson's formula. The gravity is accounted for. Since the redparticle mass is assumed constant, the particles cooled or heated by the surrounding fluid change their size; however, evaporation is not taken into account, as well as the particles' rotation, their interaction with each other

or Brown motion. When the liquid particles impact on a surface, full absorption is assumed in our simulations.

Measurements

Devices characteristics

All the experiments were conducted during 3 days (from 9 to 11 December 2020) in a clean room of IRSN, located at the CEA Saclay. The clean room is ISO 7 (NF - ISO 14-664) with a surface of 32 m^2 for which 15 m^2 were available in the central area to install the material and the participants. The average particulate concentrations in the clean room measured by an optical particle counter (OPC) Solair 3200 (size range 0.3 - 25 μm, 6 channels, measurement range $0 - 24.7.10^6$ particles/m3) sampling at 56 L/min during a preliminary qualification were 43359 $\pm$ 3902 P/m3 and 2647 $\pm$ 265 P/m3 for particles $\geq$ 0.5 μm and $\geq$ 5 μm, respectively. The measurement devices included the FIne Dust Aerosol Spectrometer (FIDAS Mobile, PALAS), providing the particle number as well as their size distribution within the particle size range from 0.18 up to 18 μm (size-segregated into 64 bins) with a time resolution of 1 Hz. The FIDAS Mobile instrument is based on optical light scattering of single particles and equipped with an optical aerosol spectrometer sensor that determines the particle size using Lorenz-Mie theory. The single particles move through an optically T-shape volume of 4.05E-06 cm^3 that is homogeneously illuminated with high-intensity white LED light source enabling a precise and unambiguous calibration curve. Each particle generates a scattered light impulse that is detected by a photo multiplier. The number of scattered light impulses gives the particle number whereas the level of the scattered light impulse gives the particle size. A condensation particle counter (ENVI-CPC 100, PALAS, single particle counting) was also deployed to measure the total number concentrations of particle from 7 nm to 5 μm with a time resolution of 1 Hz, and a cut-off diameter of 7 nm. The operating principle of the CPC is based on the magnification of particles by condensation using butanol before optical detection of the micro droplets. The sample flow rates are 1.4 and 0.9 L/min for

the FIDAS Mobile and ENVI-CPC 100, respectively. Each instrument had its own sampling line consisting of a 10 cm conductive silicone tubing (low particle separation due to electrostatic charge) connected together in a common line by a Y-funnel to transport aerosols from emission point to instrument inlets for a total tubing length of 28 cm. The set-up was also made to ensure that the distance between the sampling tube and the emission point remains constant during all measurements and doesn't impact the measured values. As a part of sanity checks, HEPA Filter was placed at the inlet of both instruments to verify a zero measurement and thus a leak check. FIDAS Mobile and ENVI-CPC total flowrates were also checked every day. Moreover, a daily calibration of the FIDAS Mobile was performed at the beginning of the day consisting in checking (and adjusting if necessary) the detector response of the analyzer by sampling a mono disperse test powder (Monodust 1500, PALAS). The sonometer used to measure the sound level was placed 50 cm in front of singers or musicians for each measurement and has been set up with a dB_A filter and rapid averaging mode.

Volunteers and set-up

The experimental study has been performed with five clarinet players with various levels of expertise and five professional singers (soprano, tenor, alto and baritone). An apparatus has been used to ensure that both clarinet and singers keep the same distance from the bell or mouth to the sampling tube. The same wooden clarinet was used for each of the five players, while each player brought his own mouthpiece and reed. References were noted down but no significant difference existed in terms of mouthpiece "overture" and reed's "strength" which are common characteristics of mouthpiece presets and reed stiffness. The distances and length of the tubes have been optimized following computations study detailed in appendix 2.

Protocol

Similar protocols have been established for clarinet playing and for singing. Both activities included five repetitions of an exercise with a protection equipment (bell cover or mask), followed by five repetitions of the exact same tasks without protection. The exercise for clarinet players consisted in playing three different notes: low E (147 Hz), B_b medium (415 Hz), and G 2^{nd} register (699Hz), at sound levels about 90±2 dB_A , monitored with a sonometer, for 10 seconds held continuously. Singers were asked to sing one single note at two sound intensities with 15 dBA difference. Singers could choose the note they were the most comfortable at, and preliminary tests were made to check whether this task could be repeated enough times by the singers. Here also, sound levels were monitored with a sonometer and notes were held continuously for 10 seconds. The singers were asked to sing only a vowel, without initial consonants in order to avoid a possible effect of increased emissions due to plosive sound. After preliminary tests on the first day to determine the time needed to reach the background level after a task, an elapsing time of 30 seconds was set between each 10-seconds task and one minute between each exercise. After 30 seconds, the concentrations went back to background levels.

Results

Computed particles emission

Clarinet with no protection at reference flow rate (10 L/min)

The computations indicate that a major part of the flow exits through the bell, with a ratio ranging from *80*% (note B♭) to *95*% (note G) and *100*% (note E, all holes closed). For the notes B♭ and G, the rest of the air tends to exit the tube through a major part of the opened keys except the register key, as shown by the velocity distribution and vectors on figure 2 for notes B♭ and G. Contrary to some other wind instruments such as saxophone or oboe, the tube of the clarinet is cylindrical, not conical. It does not enlarge, thus fostering the exit of air through holes. The register key is specific, since a small pipe emerges

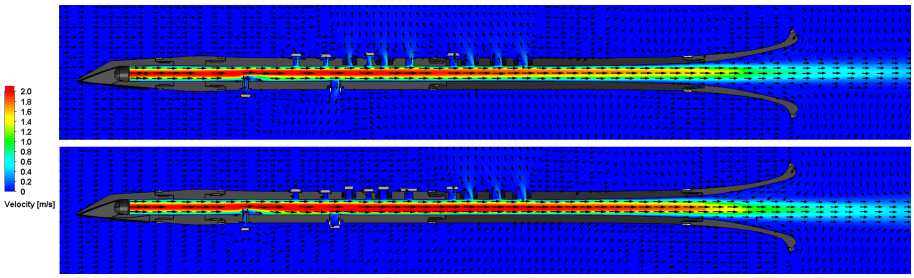

Figure 2: Air velocity contours and vectors in a section plane of the clarinet - notes B♭ (top) and G (bottom)

in the main tube; this prevents the flow from exiting through it, even in opened position. Downwards this pipe, the flow is perturbed as revealed by the low velocity area on the figure 2. In the bell, the air jet remains concentrated, surrounded by vortices at the outlet. Its direction is slightly deviated downwards for note G, while remaining centered for note B♭ probably due to the opening of the thumb key on the opposite side of the majority of toneholes. In reality, the mixing layer at the boundary of the outcoming jet would lead to eddies, that cannot be numerically captured solving averaged flow equations as performed here. Such eddies are clearly shown on Schlieren imaging by Becher *et al.* [7] for example.

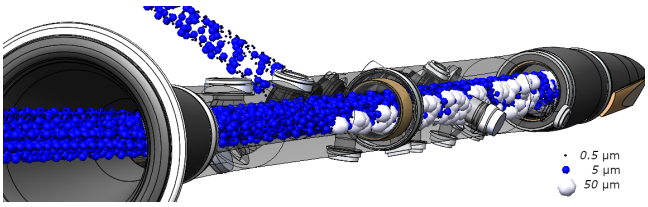

Figure 3: Trajectories of droplets with respect to their diameters, as seen from the bottom (note G)

As shown in Table 1a, the computations of droplets trajectories in the clarinet indicate a deposit of small and medium droplets on internal walls by 1 to 12% with respect to the played note, and exit through toneholes by up to 23%.

Instrument fingerings	E	G	B♭	Whatever
Exit of air through keys	0%	5%	20%	-
Exit of air through bell	100%	95%	80%	-
Droplet diameter	0.5-5 μm	0.5-5 μm	0.5-5 μm	50 μm
Total deposit	1%	7%	12%	100%
Exit through keys	-	12%	23%	0%
Exit through bell	99%	81%	65%	0%

(a) Without protection

Instrument fingerings	E	G	B♭	Whatever
Exit of air through keys	0%	79%	83%	-
Exit of air through bell	100%	21%	17%	-
Droplet diameter	0.5-5 μm	0.5-5 μm	0.5-5 μm	50 μm
Total deposit	8%	31%	31%	100%
Exit through keys	-	50%	54%	0%
Reach bell protection	92%	19%	15%	0%

(b) With protection

Table 1: Computed rates of droplet behaviors in clarinet with respect to played music note and droplet diameter, without and with protection at the bell, at a flowrate of 10 l/min

The ratio increases with the number of opened keys. A large majority of the small and medium droplets reaches the bell, by 65 to 99% while toneholes are progressively closed. The sum of the ratio for deposit and exit through bell is slightly below the ratio of air flow at the bell, by 7% for note G and 3% for note B♭. This is only partially due to the deposit on the internal face of opened keys (for about 1%), indicating that particles tends to exit through keys more easily than air. The trajectories are similar for both small and medium droplets; on the contrary, larger droplets all deposit due to gravity (Figure 3).

Effect of protection

The effect of the bell cover on the air flow is illustrated on figure 4 for notes E and G. When all toneholes are closed and the only possible way out is the bell (note E), the jet remains concentrated in the bell and enlarges just right upstream the protection. The latter prevents the external air from entering inside, leading to aerodynamic dead zone in the volume between the jet and

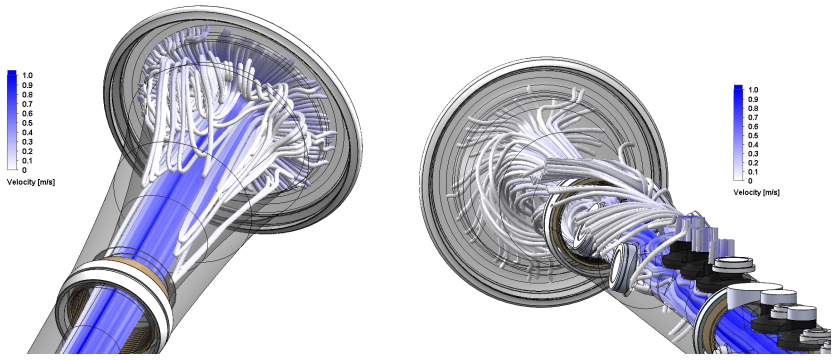

Figure 4: Streamlines upstream the bell cover for note E (left) and G (right)

the wall. When some toneholes are opened, the air flow exiting through the bell is drastically reduced, to 21% (note G) or 17% (note B♭) of the injected flowrate, for the benefit of flows through toneholes. As a consequence, the droplets trajectories are also drastically modified (Table 1b). The deposit of small and medium droplets is at least tripled compared to the case without bell cover. For the two played notes with partially opened keys, the proportions are now similar: half of the droplets exits through keys, one third deposits on walls while only 15% to 19% reach the protection. Large droplets still all deposit in the inner part f the instrument. Currently, it is not possible to establish that particles can cross the bell cover or not.

Effect of flow rate

The ratio of flow rate passing through the bell cover remains almost unchanged when the inlet flow rate is decreased from 10 l/min to 7.5 l/min or increased up to 12.5 l/min. It stays close to 21% at 7.5 l/min and is slightly lowered to 20% at 12.5 l/min. The effect of flow rate on particle trajectories has been numerically investigated for note G with bell cover. Results are given in table 2. The ratio of particles exiting through keys increases by 1 point or 2 points at the lowest flow rate, as does the air flow. The amount of particles reaching the bell protection tends to decrease by 3 points at the highest flow rate, to the benefit of deposit. The behavior of small particles starts to differ-

entiate from the one of medium particles only at the smallest flow rate. The deposit is then lowered since the small particles tend to follow the flow, exiting through keys (+2 points) or reaching the bell protection (+1 point).

Flowrate	7.5 l/min		10 l/min		12.5 l/min	
Droplet diameter	0.5 μm	5 μm	0.5 μm	5 μm	0.5 μm	5 μm
Total deposit	27%	30%	31%	31%	33%	34%
Exit through keys	53%	51%	51%	50%	51%	50%
Reach bell protection	20%	19%	18%	19%	16%	16%

Table 2: Computed rates of droplet behaviors in clarinet with respect to flowrate and droplet diameter, with protection at the bell, for note G

Measurements results

Played note effect on particle concentration and size

The particle concentration for clarinet players and three different notes with and without protection is given as box and whisker plots in the fig. 5 and 6 for respectively CPC and FIDAS. Mean particle concentration was calculated for each played note and averaged over the 10 seconds duration for all the assays. Without any protection on the instrument bell, the played note plays an important role on the particle emission. Both CPC and FIDAS Mobile generally counted more particles for E note than for Bb and G even though a large variability between players is observed. Concentration-wise, the order of emission is E > Bb > G for CPC measurements while Bb and G showed similar particle concentration on the FIDAS Mobile measurements. The number size distribution, only given by the FIDAS Mobile analyzer, is generally centered around 300 nm, whatever the played note. It is however important to note that the d50 might be shifted to larger diameters compared to the real d50 due to the fact that the FIDAS is not counting particles smaller than 180 nm which might be present in samples. Comparing concentration levels between both devices indicates a 10 to 20 ratio between $[7.10^{-3}; 5]\mu m$ and $[0.18; 18]\mu m$, thus suggesting a majority of particles below 0.180 μm.

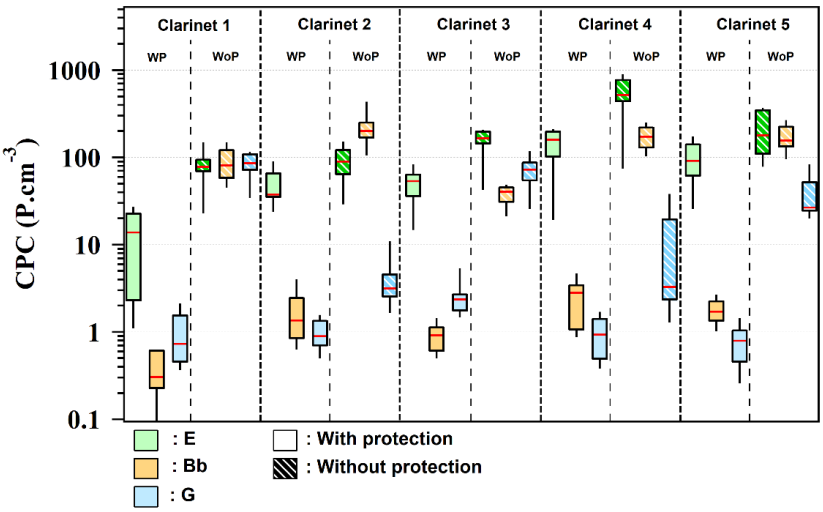

Figure 5: Particle concentration measured with the butanol-CPC. The green, orange and blue boxplots represent the E, Bb and G notes, respectively. The plain and dashed boxplots represent the assays with (WP) and without (WoP) protection. The red line is the median value.

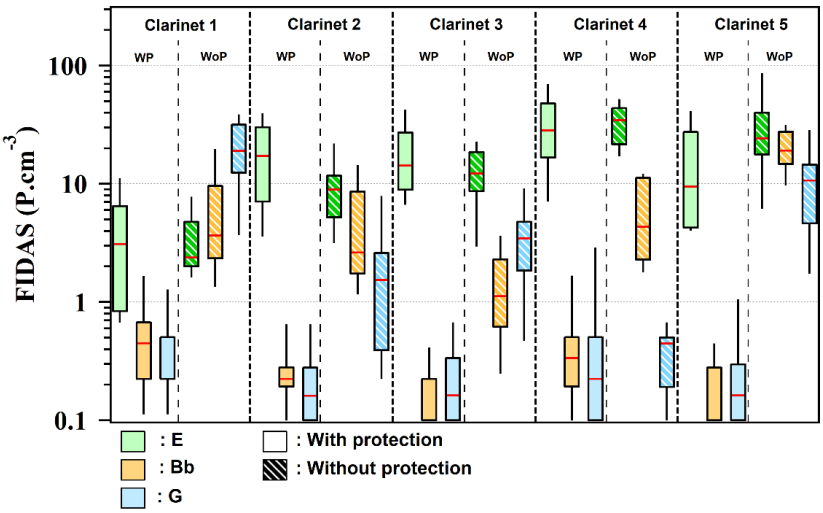

Figure 6: Particle concentration measured with the FIDAS Mobile. The green, orange and blue boxplots represent the E, Bb and G notes, respectively. The plain and dashed boxplots represent the assays with (WP) and without (WoP) protection. The red line is the median value.

Measurement device		FIDAS			CPC		
Note		E	Bb	G	E	Bb	G
With protection [P/cm^3]	μ	14.5	0.3	0.2	71.3	1.4	1.1
	σ	9.4	0.1	0.1	57.0	1	0.7
	COV [%]	64	33	50	80	71	64
Without protection [P/cm^3]	μ	16.5	6.2	5.2	207.0	130.4	38.2
	σ	12.8	7.3	7.8	181.7	67.4	38.8
	COV [%]	77	118	150	88	52	102
p-value (N=25) W & W/O protection	[-]	0.53	2.0e-4	2.4e-3	8e-4	1e-4	1e-4

Table 3: Particle concentration measured on clarinet with the two devices with and without protection, mean μ, standard deviation σ and coefficient of variation COV. P-value is given as statistical significance when comparing with and without protection populations.

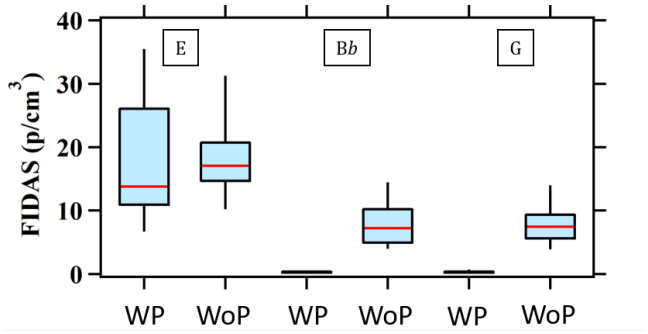

(a)

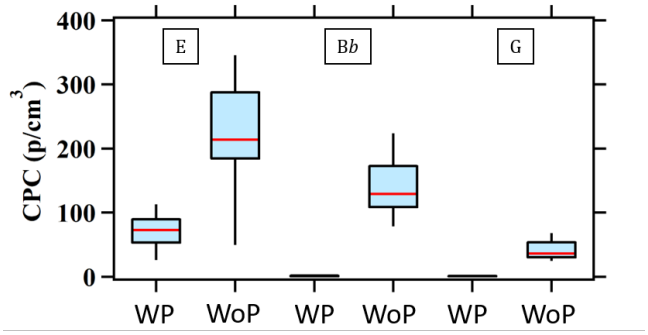

(b)

Figure 7: Boxplots of particle concentration averaged for all the clarinettists. (a) FIDAS, (b), CPC

Clarinets protection effect on particle emission and size

The bell protection consisted in a 2-layered tissue made of 40 % cotton and 60 % viscose on the outside and 100 % polyester on the inside part. It was equipped during the first series of clarinet assays. The ratios between the measurements with (WP) and without (W/O P) were calculated for each note. For the Bb and G notes measured by the FIDAS Mobile analyzer, the reduction ratio was rather similar (36 and 29), respectively. For the CPC, these ratios were respectively 122 and 38.

Interestingly, the E ratios are 1.2 and 3.3 for FIDAS Mobile and CPC, respectively whereas the particle emissions are in the same order of magnitude. The particle concentration when the protection is equipped is much higher than the background concentration for both measurement devices and for all the clarinetists.

When playing with the bell cover the note E, i.e. when all the tone holes are closed, measured concentration levels are much higher than the other notes with protection and rather range in the same order of magnitude than when playing without protection, both on FIDAS and on CPC. While on the CPC median values for E are still clearly lower with protection than without, it is not the case for the FIDAS measurements, where two clarinet players (clarinet 2 and clarinet 3) have higher emissions with protection than without.

Figure 8 (a) shows the size distribution for particles measured by the FIDAS, i.e. in the range 180 nm - 18 μm, for the 5 clarinet players and grouped by note. In this size range, median sizes are 224, 227 and 293 nm for E, Bb and G, respectively. However, it should be kept in mind that these distributions and median values would shift to finer sizes if counting also the particles measured on the CPC's size range. Moreover, looking at the number concentrations measured by each device for the essays without protection, we can see an important ratio between the CPC and FIDAS, which shows much higher concentrations in the CPC's size range. An explanation for this observation is provided in the discussion section. There is approximately a factor 10 between mean number

concentrations measured by the CPC and the FIDAS (12.5 factor for E, 21 for Bb and 7.3 for G).

E was the only note on which a sufficient number of particles was measured to allow representing the size distribution WP. The figure 8 (b) shows a more concentrated peak for measurements WoP, while values measured WP are more widespread and present more particles $>$ 300 nm compared to WoP. Median sizes are 224 and 302 respectively for the note E WoP and WP.

Measurement device	FIDAS			CPC		
Note	E	Bb	G	E	Bb	G
$\mu \pm 1\sigma$	1.2 ± 0.8	35.6 ± 56.9	29.2 ± 32.7	3.3 ± 1.4	121.9 ± 88.9	37.6 ± 46.5

Table 4: Particle concentration reduction efficiency of the bell cover, mean μ and standard deviation σ

Particle concentration and sizes for singers

The particle concentration for singers with two sound levels measured with the FIDAS and CPC devices are given as box and whisker plots in the fig 9 and 10 respectively. Without mask, the particle concentration ranges between 0.2 and 150 [P/cm^3] for FIDAS and between 1 and 90 [P/cm^3] for CPC (for extreme values and different loudness). Considering the average values, the particle concentration ranges between 0.8 and 80 [P/cm^3] for FIDAS and between 2 and 70 [P/cm^3] for CPC, taking into account both low and high loudness.

Singing loudness on particle emission and size

Mean particle concentration was calculated for each singer and averaged over all the assays. The results are shown in table 5. When we consider the "W / O P" conditions, it clearly appears that the increasing voice loudness has an increasing impact on the measured particle concentration for both measurement devices. It is also obvious that the data variability among singers is significant. The increasing ratio between the "Low" and "High" conditions depend and are equal to 7.4 and 3.0 for FIDAS Mobile and ENVI-CPC, respectively.

The similar mean concentrations measured by the two measurement devices

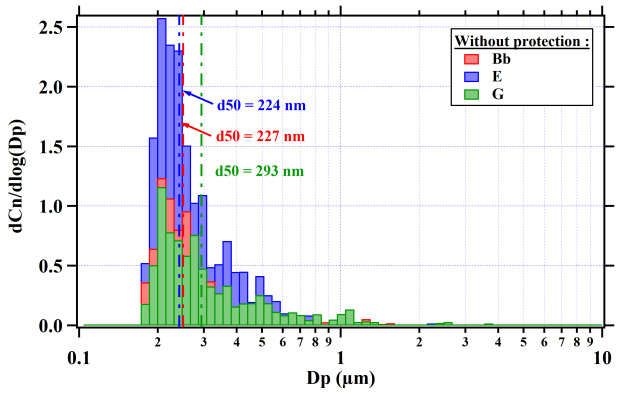

(a)

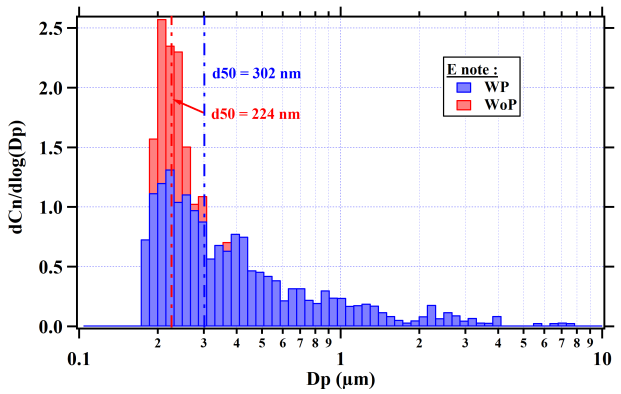

(b)

Figure 8: Size distribution of particles for (a) three notes without protection, (b), E not with and without protection

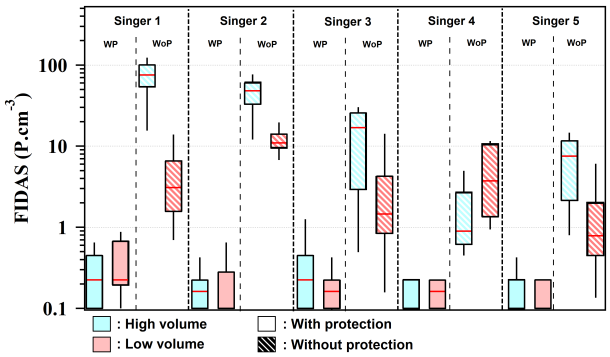

Figure 9: Particle concentration measured with the FIDAS Mobile. The light blue and red box plots represent the high and low volumes, respectively. The plain and dashed box plots represent the assays with (WP) and without (WoP) protection. The red line is the median value.

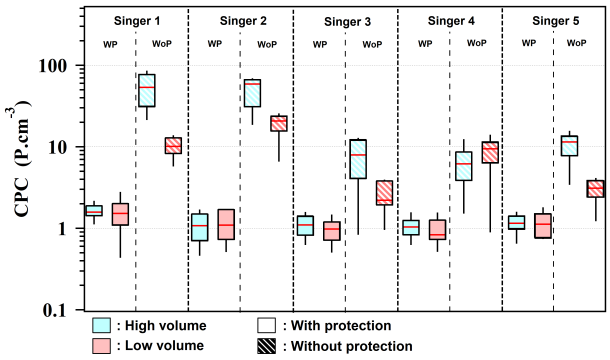

Figure 10: Particle concentration measured with the butanol-CPC. The light blue and red box plots represent the high and low volumes, respectively. The plain and dashed box plots represent the assays with (WP) and without (WoP) protection. The red line is the median value.

shows that the particle size should be higher than 180 nm (lower boundary of FIDAS Mobile). The calculated median diameter for "Low" and "High" conditions are 307 and 313 nm, respectively, indicating that there is no influence of the loudness in these conditions on the exhaled particle size. It is important to note that the mean diameter is calculated using number concentration instead of mass concentration used in some other studies.

Device		FIDAS (P/cm^3)		CPC (P/cm^3)	
Loudness		High	Low	High	Low
W/Protection	μ	0.2	0.15	1.2	1.1
	σ	0.05	0.05	0.2	0.2
	COV [%]	25	33	17	18
W/O Protection	μ	29.8	4.0	27.6	9.1
	σ	28.0	3.6	23.5	6.6
	COV [%]	94	90	85	72
p-value	[-]	10-4	10-4	10-4	10-4

Table 5: Particle concentration measured on singers with the two devices with and without masks, mean μ, standard deviation σ and coefficient of variation. Statistical significance between each case.

Protection effect on particle emission and size

The surgical 3-layered mask was equipped during the second series of assays. The protocol was identical between assays with and without protection. Looking at the table 6, wearing a surgical mask does have a significant impact on the measured particle concentration. It is however crucial to note that the sampling point was placed directly in front of the singer's mouth, therefore the instruments do not take the side leaks into account. As explained previously, the decrease in particle number concentration is more important with the FIDAS Mobile than the ENVI-CPC.

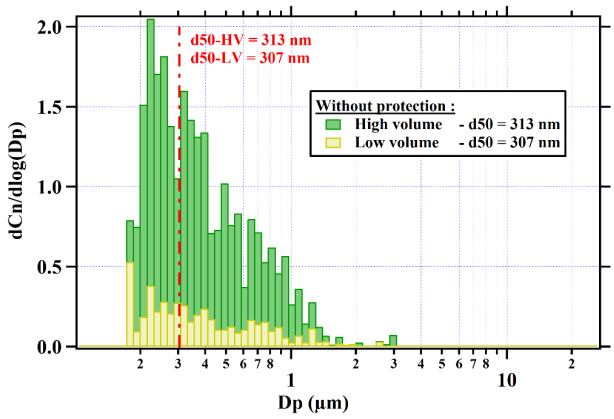

(a)

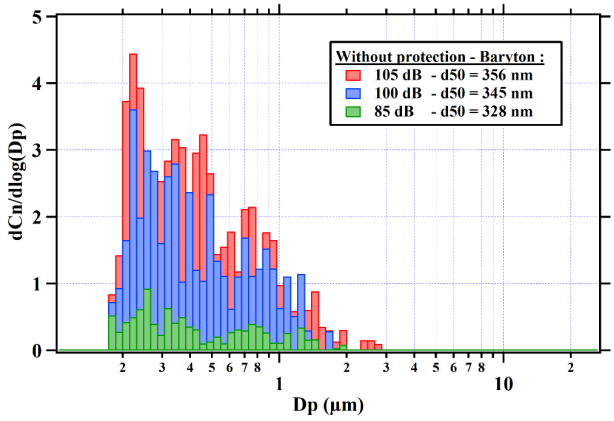

(b)

Figure 11: (a) Particle number size distribution measured by FIDAS Mobile for "Low" and "High" conditions without mask, (b) particle number size distribution measured by FIDAS Mobile for 3 different loudness conditions for one singer without mask. The sung note is an A4.

Instrument	FIDAS Mobile		ENVI-CPC	
Loudness	High	Low	High	Low
$\mu \pm 1\sigma$	174 ± 170	26.5 ± 25	23.6 ± 20.5	8.3 ± 6.3
P value	10-4		10-3	

Table 6: Calculated ratios for both measurement device between "WP*" and "W/O P" conditions. The values presented here are the average for all the singers.

Discussion

Inter- and intra-individual variability Without protection

Clarinets

Coefficients of variation obtained for clarinet without protection vary between 52 and 150 % depending on the note played and the measuring device. Looking at 3, we can see that even though E seems to be the most emitting note in general on both size ranges without protection, this tendency was not clear for all five players. The distinction between Bb and G was highly variable. We can also observe that for some conditions, there was one order of magnitude between the 1st and 3rd quartile of a same note played by the same musician, though this gap is generally smaller.

Two phenomena could justify the larger amount of particles measured for some cases : (i) more particles are injected into the instrument, i.e. a higher generation of particles takes place at the mouthpiece, and/or (ii) for a same amount of particles generated at the mouthpiece, the pathways of the particles can be different and the number of particles sampled at the bell can be decreased by both deposition on the instrument's inner walls and by air flows escaping through tone holes. It would be interesting to make measurements on several clarinet players by sampling directly at the mouthpiece in order to evaluate the importance of (i).

Phenomenon (ii) was assessed through CFD results which allow estimating the number of particles that would reach the bell depending on the fingering, for identical flow rate and amount of particles injected at the mouthpiece, and for varying flow rates. Few essays were made with increasing loudness and showed an important increase in number concentration measured. Many factors could affect the amount of particles measured. Looking at the generation of particles at the mouthpiece, we can imagine the effect of liquid accumulation both in the musician's mouth and on his reed, which vibration will stretch-up then break the saliva filaments between the reed and the mouthpiece, as visualized by [21] on a saxophone's mouthpiece. The act of playing involves deep inspirations

coming from the lower respiratory tracts.
The effort made by musicians (and subsequent leaks at mouth) to keep a note for 10 seconds at a given intensity can vary according to their level of expertise, tiredness, etc. and induce varying emissions. Another fact linked to temporal questions would be the level of humidity in the instrument, both the relative humidity of the air inside the tube, and the surface humidity of the tube. CFD modelizations suggest the importance of deposition of particles in the tube, which can be seen easily: the bore tends to be wet and to form a small channel flowing down to the bell and dropping out. The phenomenon of re-aerosolization is not well characterized yet but the possibility of re-suspending particles gathered in a liquid form due to the air velocity (not exceeding 2 m/s inside the bore according to our CFD) remains an open question.

Singers

Coefficients of variation for the 5 singers without protection range from 72 to 94 %, as given in table 5. Protocols have been defined in order to make the most repeatable essays as possible. Distances and tube length were minimized and fixed, no consonants were pronounced and sound level was monitored, leading to the least variability possible, which can explain that the variation observed is less than for most conditions on the clarinet. The bias explained above about clarinet (humidification of the instrument, flow rate at the mouthpiece) may not be applicable for these measurements.

Concentrations and sizes of particles emitted without protection - comparison to existing state of the art

Clarinet

The presented measurements with clarinets without protection led to an average concentration from 5.2 to 15.5 particles per cm^3 on the FIDAS and from 38.2 to 207 particles per cm^3, depending on the notes played with a coefficient of variation between 52 and 150 %. Data from the state of the art suggest

concentrations approaching 2 or more particles per cm^3 according to [15], the latter value appointing the maximal peak reached during a four-minutes play. In both studies, these values were measured by APS in the size range (0,5 to $20\mu m$) at the bell of the clarinet. To compare our data to literature, we applied a cut-off on the FIDAS reported values to count only particles between 0,5 and $20\mu m$and got average concentrations for the 5 clarinetists between 0,75 and 1,21 particles per cm^3 (for Bb and G respectively).

It should be noted that the protocols, environmental conditions, sampling devices, actions asked to musicians, are various and can have a direct impact on the amount, and particularly on the size of the measured particles. [14] estimates the size of particles to follow a log normal distribution with averages between 1.9 and 3.1 μm depending on the instrument, clarinet having a mean size about 2,5 μm. This value is obtained using a calibration between APS and DIH (Digital In-line Holography) devices and through amplifying ratio, thus potentially overestimating the size of the particles at the sampling point. The calibration was conducted by applying both APS and DIH to measure the aerosols generated by a nebulizer (TSI Single Jet Atomizer 9302) under different back-pressure conditions. Our findings are however consistent with [15] which reports a majority of particles under 2.5 μm and a high number of submicronic particles for the clarinet which might probably be dry residues (droplet nuclei after evaporation process).

Singers

The presented measurements with unmasked singers led to average concentrations between 4 and 28 particles per cm^3 on the FIDAS for the 5 singers and for low and high volume, respectively. CPC measured the same orders of magnitudes. Emitted concentrations turned out to be highly dependant on vocal loudness, in agreement with [10], [11] and [17] on singers, as well as with [13] on speech.

The mean size of our measurements on singers, following log-normal distribution (see fig.11) is between 307 and 313 nm depending on sound level. Particles

above 1 μm are very scarce for loud singing and almost zero for low intensity. The predominance of submicronic particles while singing was also highlighted by [11], [17] [18] [10], with different amounts of particles > 1 μm ; this difference being possibly due to varying sampling methods and the tasks asked to the singers.

Concentrations and sizes of particles emitted with masks and bell covers - comparison to existing state of the art

Both the surgical mask and the bell cover turned out to effectively reduce the amount of particles measured, on the two measured size ranges. Coefficients of variation have shown a steep decrease between without protection and with protection.

The averaged reduction ratio with surgical mask is comprised between 8 and 20 on the CPC device and is higher for higher sound levels. Other studies did measurements on singers wearing a surgical mask and reported decreases of the mean particle rates from 980 to 410 particles/second for loud singing [11] and from 10 to 0,2 particles/seconds for speaking [22].

However, [18] showed by measuring emission rates at different points around the mask that important leakage occured when talking through a surgical mask, with about 10 times more particles measured above the nose than in front of the mouth. Total efficiency should therefore consider emissions' reduction through the mask, but also on the sides and above the mask.

The averaged reduction ratio measured in our works with bell cover is between 3.3 and 121.9, depending on devices and notes played. The mean reduction factors were much higher on the CPC than on the FIDAS (see fig.4) and were very small on the E, whatever the device, compared to G and Bb. For clarinets 1, 2 and 3, the mean concentration on FIDAS for the note E is even higher WP than WoP. The same was observed by [22] when singing with home-made cloth masks, with higher total particle rates when wearing the mask and especially an enhanced contribution of large particles due to fiber shedding. Looking at the granulometry WP and WoP, we can suppose that when closing all the

tone holes (fingering of note E) and thus forcing the air to go through the bell cover rather than escaping elsewhere, the air flows carries some fibers from the cloth. Bell cover was observed to get partially wet after a certain time of playing and the phenomenon of humidification of the fibers could be explored in order to determine whether re-aerosolization of the particles deposited on the cover could occur and might explain a higher number of particles measured on the E WP. Bell covers with different compositions have been studied by [15] and [23]. [15] found out that playing with a surgical mask fixed at the bell of a clarinet reduced the measured concentrations to background level while [23] placed a speaker cloth with 1, 2 or 3 layers at a trumpet's bell and calculated a filtration efficiency of 60 %, 70 % and 90 %, respectively.

Conclusion

This study highlighted the strong inter and intra-individual variability, which is associated with individuals characteristics and technique, sound level, fingerings and tone holes opening. The reduction means have proven useful. For bell cover, their reduction ratio is statistically significant for almost all notes and devices, especially for small particles. For clarinets, most of the big sizes particles are firstly filtered by deposition in the instrument, as well as smaller particles whose total exit proportion outside the instrument is lower. Such method can be an additional protection with positive outcomes. The predominance of very fine particles in the case of the clarinet leads to interrogations about to what extent these emitted particles could lead to a risk of transmission, the SARS-CoV-2 virus being estimated to measure 100 nm. For singers, whose measurements were performed in front of the mouth, masks have proven useful and are efficient for each sound level and singers. Most of the particles measured had sizes lower than $1\mu m$, therefore we can wonder to what extent such particles would be able to carry some infectious viruses.

References

[1] W. H. Organization, Transmission of SARS-CoV-2 : implications for infection prevention precautions: scientific brief, 09 July 2020 (July) (2020) 1–10.

[2] M. Jayaweera, H. Perera, B. Gunawardana, J. Manatunge, Transmission of COVID-19 virus by droplets and aerosols : A critical review on the unresolved dichotomy Transmission of COVID-19 virus by droplets and aerosols : A critical review on the unresolved dichotomy (June) (2020). doi:10.1016/j.envres.2020.109819.

[3] M. R. Moser, T. R. Bender, H. S. Margolis, G. R. Noble, A. P. Kendal, D. G. Ritter, An Outbreak Of Influenza Aboard A Commercial Airliner, Journal of Epidemiology 110 (1) (1979). doi:10.1093/aje/155.5.478. URL http://joi.jlc.jst.go.jp/JST.JSTAGE/jea/17.194?from=Google

[4] S. Yezli, J. A. Otter, Minimum Infective Dose of the Major Human Respiratory and Enteric Viruses Transmitted Through Food and the Environment, Food and Environmental Virology 3 (1) (2011) 1–30. doi:10.1007/s12560-011-9056-7.

[5] C. J. Kähler, T. Fuchs, R. Hain, Can mobile indoor air cleaners effectively reduce an indirect risk of SARS- CoV-2 infection by aerosols ? Can mobile indoor air cleaners effectively reduce an indirect risk of SARS-CoV-2 infection by aerosols ? (August) (2020) 1–24. doi:10.13140/RG.2.2.14081.68963.

[6] P. De La Cuadra, C. Vergez, B. Fabre, Visualization and analysis of jet oscillation under transverse acoustic perturbation, Journal of Flow Visualization and Image Processing 14 (4) (2007) 355–374. arXiv:arXiv:0811.0333v1, doi:10.1615/JFlowVisImageProc.v14.i4.20.

[7] L. Becher, A. W. Gena, H. Alsaad, B. Richter, C. Spahn, C. Voelker, The spread of breathing air from wind instruments and singers using schlieren techniques, Indoor Air (2020) (2021). doi:10.1111/ina.12869.

[8] I. M. Viola, B. Peterson, G. Pisetta, G. Pavar, H. Akhtar, F. Menoloascina, E. Mangano, K. E. Dunn, R. Gabl, A. Nila, E. Molinari, C. Cummins, G. Thompson, C. M. McDougall, T. Y. M. Lo, F. C. Denison, P. Digard, O. Malik, M. J. G. Dunn, F. Mehendale, Face Coverings, Aerosol Dispersion and Mitigation of Virus Transmission Risk (May) (2020). arXiv:2005.10720.
URL http://arxiv.org/abs/2005.10720

[9] A. Abraham, R. He, S. Shao, S. S. Kumar, C. Wang, B. Guo, M. Trifonov, R. G. Placucci, M. Willis, J. Hong, Risk Assessment and Mitigation of Airborne Disease Transmission in Orchestral Wind Instrument Performance, medRxiv 157 (April) (2020) 105797. doi:10.1101/2020.12.23.20248652.
URL https://doi.org/10.1016/j.jaerosci.2021.105797

[10] F. K. A. Gregson, N. A. Watson, C. M. Orton, A. E. Haddrell, L. P. Mccarthy, T. J. R. Finnie, N. Gent, G. C. Donaldson, P. L. Shah, Comparing the Respirable Aerosol Concentrations and Particle Size Distributions Generated by Singing , Speaking and Breathing 2 1–27.

[11] M. Alsved, A. Matamis, R. Bohlin, M. Richter, P. E. Bengtsson, C. J. Fraenkel, P. Medstrand, J. Löndahl, Exhaled respiratory particles during singing and talking, Aerosol Science and Technology 54 (11) (2020) 1245–1248. doi:10.1080/02786826.2020.1812502.
URL https://doi.org/10.1080/02786826.2020.1812502

[12] D. Mürbe, M. Fleischer, J. Lange, H. Rotheudt, M. Kriegel, Aerosol emission is increased in professional singing (2020) 1–10.

[13] S. Asadi, A. S. Wexler, C. D. Cappa, S. Barreda, N. M. Bouvier, W. D. Ristenpart, Aerosol emission and superemission during human speech increase with voice loudness, Scientific Reports 9 (1) (2019) 1–11. doi:

10.1038/s41598-019-38808-z.
URL http://dx.doi.org/10.1038/s41598-019-38808-z

[14] R. He, L. Gao, M. Trifonov, J. Hong, Aerosol Generation from Different Wind Instruments, medRxiv (September) (2020) 2020.08.03.20167833. doi:10.1101/2020.08.03.20167833.
URL http://medrxiv.org/content/early/2020/08/07/2020.08.03.20167833.abstract

[15] T. Stockman, S. Zhu, A. Kumar, L. Wang, S. Patel, J. Weaver, M. Spede, D. Milton, J. Hertzberg, D. Toohey, M. Vance, J. Srebric, L. Shelly, O. Sciences, Measurements and Simulations of Aerosol Released while Singing and Playing Wind Instruments.

[16] L. P. McCarthy, C. M. Orton, N. A. Watson, F. K. A. Gregson, A. E. Haddrell, W. J. Browne, J. D. Calder, D. Costello, J. P. Reid, P. L. Shah, B. R. Bzdek, Aerosol and Droplet Generation from Performing with Woodwind and Brass Instruments, Aerosol Science and Technology 0 (0) (2021) 1–11. doi:10.1080/02786826.2021.1947470.
URL http://dx.doi.org/10.1080/02786826.2021.1947470

[17] D. Mürbe, M. Kriegel, J. Lange, L. Schumann, A. Hartmann, M. Fleischer, Aerosol emission of adolescents voices during speaking, singing and shouting, Plos One 16 (2) (2021) e0246819. doi:10.1371/journal.pone.0246819.

[18] C. D. Cappa, S. Asadi, S. Barreda, A. S. Wexler, N. M. Bouvier, W. D. Ristenpart, Expiratory aerosol particle escape from surgical masks due to imperfect sealing, Scientific Reports 11 (1) (2021) 1–12. doi:10.1038/s41598-021-91487-7.
URL https://doi.org/10.1038/s41598-021-91487-7

[19] S. Asadi, C. D. Cappa, S. Barreda, A. S. Wexler, N. M. Bouvier, W. D. Ristenpart, Efficacy of masks and face coverings in controlling outward

aerosol particle emission from expiratory activities, Scientific Reports 10 (1) (2020) 1–13. doi:10.1038/s41598-020-72798-7.
URL https://doi.org/10.1038/s41598-020-72798-7

[20] Simcenter, Simcenter FLOEFD Technical Reference, Software version 2020.2 (2020).

[21] M. Abkarian, H. A. Stone, Stretching and break-up of saliva filaments during speech: A route for pathogen aerosolization and its potential mitigation, Physical Review Fluids 5 (10) (2020) 1–10. doi:10.1103/PhysRevFluids.5.102301.

[22] C. D. Cappa, W. D. Ristenpart, S. Barreda, N. M. Bouvier, A. S. Wexler, S. A. Roman, Title : An improved and highly efficient geometry for facemasks.

[23] A. Abraham, R. He, S. Shao, S. S. Kumar, C. Wang, B. Guo, M. Trifonov, R. G. Placucci, M. Willis, J. Hong, Risk assessment and mitigation of airborne disease transmission in orchestral wind instrument performance, Journal of Aerosol Science 157 (April) (2021) 105797. doi:10.1016/j.jaerosci.2021.105797.
URL https://doi.org/10.1016/j.jaerosci.2021.105797

[24] W. A. Sirignano, Fluid Dynamics and Transport of Droplets and Sprays, Cambridge University Press, 1999. doi:10.1017/CBO9780511529566.

Acknowledgments

This study was performed in the frame of the project PIC / PIV (Protocoles pour les Instruments face au Coronavirus / Pratique Instrumentale et Vocale) involving Chambre Syndicale de la Facture Instrumentale – CSFI, Institut technologique Européen des Métiers de la Musique – ITEMM, and Les forces musicales. Individual informed consent was obtained for measurements where musicians and singers were playing/singing. Authors acknowledge the following funders and support : Ministère de la culture, Fondation Bettencourt Schueller, Audiens, Région Ile de France, La Direccte. ITEMM is an innovation pole supported by Le Mans Métropole, Direction Générale des Entreprises, Région Pays de la Loire, and DRAC Pays de la Loire.

Appendix

Impact of sampling method on particles measurements

The life time of liquid droplet may be expressed as [24]:

$$\tau_{ev,d^2} = \frac{\rho_l}{\rho_g} \frac{d^2}{4 D_g Sh_g ln(1 + B_M)} \tag{1}$$

with ρ_l the liquid density, ρ_g the gas density, d the droplet diameter, D_g the diffusivity in gaseous phase, Sh_g the Sherwood number, B_M the mass Spalding number calculated from the mass fraction of vapor in ambient air (of relative humidity below 100%) and from the droplet surface (of relative humidity equal to 100%). Applying this formula to water droplets, with a Schmidt number of 1 for the calculation of the diffusivity and a Sherwood number equal to 2, leads to the evaporation times as given in table 7. Therefore pure water droplets with a diameter below 50 μm evaporate very quickly, in less than half a second. The FIDAS 6 mm diameter sampling tube having a flow rate of 1.4 L/min, its length has been taken as short as possible, namely 30 cm, leading to a travel time of 360 ms. However, in such conditions, it is clear that droplets measured with diameters below 20 μm are dry residuals of initially partially liquid saliva droplets.

Droplet diameter [μm]	5	20	30	50	80	100
Evaporation time [ms]	10	70	150	410	1 050	1 640

Table 7: Life time of water liquid droplets at $26°C$ and 50% relative humidity

Pulmonary ventilation of woodwind players and singers

The pulmonary ventilation measurements have been performed to evaluate particles emission rate from particles concentration, for different musicians and singers. The musicians perform two tasks during one minute by either singing in an respiratory mask or using their mouthpiece, connected with a tube. The tube is associated with a Gallus, a gas meter device that measures the flow rate. The Gallus sensitivity is equal to 0.1 dm^3. The results are given in the table 8.

Table 8: Pulmonary ventilation rate (PVR) for different musicians and tasks

Instruments or voice	**PVR Average** [$\frac{m^3}{h}$]	**PVR standard deviation** [$\frac{m^3}{h}$]
Clarinet	0.6	0.2
Oboe	0.2	0.03
Saxophone	0.9	0.2
Trumpet	0.6	0.07
Flute	0.6	0.09
Tuba	1.6	0.1
Woodwinds mixed	0.7	0.4
Sopranos	0.4	0.1
Baryton	0.5	0.15
Tenor	0.3	0.17
Alto	0.4	0.13
Singers mixed	0.4	0.14

Clarinet fingerings

The fingerings used for clarinet are given the figure 12.

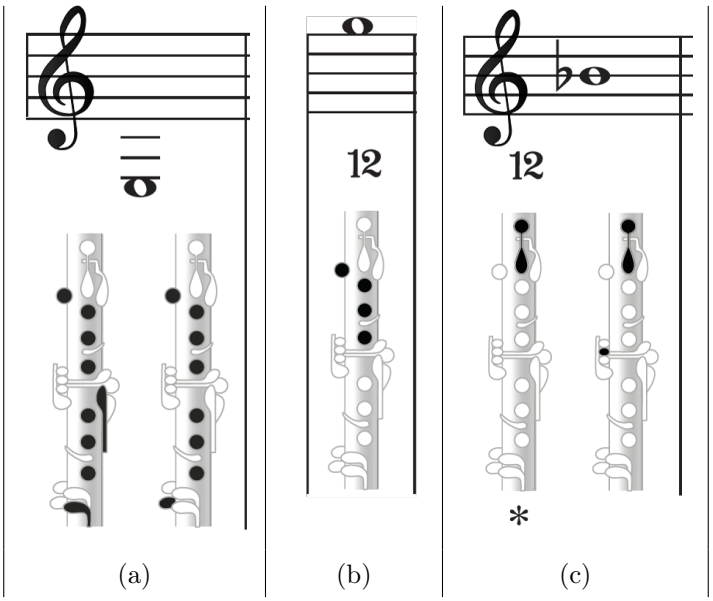

Figure 12: Considered fingerings for clarinet ; (a), note E ; (b), note G, (c), note B♭

Numerical validation

Further analysis is proposed here to evaluate the reliability of the computations. It is applied on the case of the clarinet. Regarding the mesh, it is automatically computed, although manually tuned to achieve targeted cell sizes. It uses a Cartesian meshing technology, meaning that cells are cubic. Local refinement is achieved by progressively cutting cells by two in all directions up to the targeted cell sizes (octree technique). The nominal mesh contains 0.6 million cells. The basic cell size is 15 mm. It is increased by a factor of 3 in the far field. On the opposite, it is refined so that the mesh contains at least 10 cells in all cross-sections (tube, tone-holes). It is also refined up to 5 times close to walls, reaching 0.5 mm at the wall. For the considered flow rate, the y^+ ranges from 4 close to the injection plane to 0.5 at the bell inlet. It is therefore below 5, allowing for the resolution of the viscous sub-layer instead of its modeling through the use of wall laws. Two other meshes have been investigated for mesh convergence analysis: a coarser mesh and a finer one. They are basically obtained by multiplying or dividing, respectively, the basic cell size by a factor

of 2. For the coarse mesh however, cell size is maintained at walls to the same level as in the basic mesh, in order to ensure satisfactory y^+. The table 9 gives a sum up of the values.

Table 9: Mesh characteristics

Level	**Total number of cells**	**Number of partial fluid/solid cells**	**Cell size at wall**	**Range of y^+**
Coarse	170 000	90 000	0.50 mm	[0.50-4]
Nominal	600 000	180 000	0.50 mm	[0.50-4]
Fine	2 800 000	470 000	0.25 mm	[0.25-2]

The figure 13 shows the evolution of the ratio of air coming out through the bell feature with respect to the mesh size values.

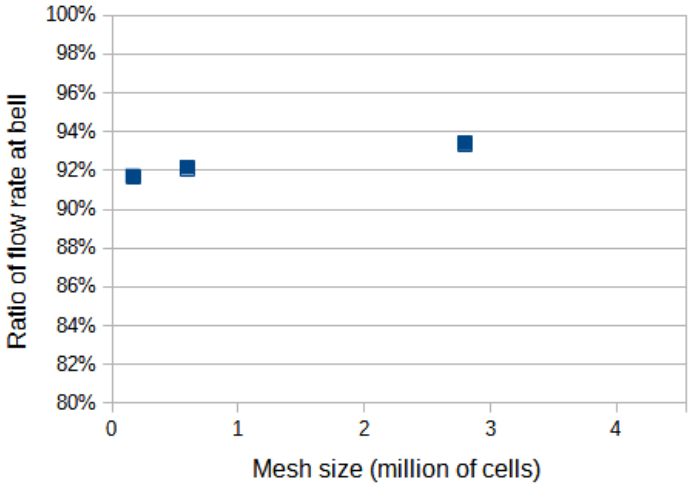

Figure 13: Flow rate at the bell with respect to mesh size for clarinet

Since the discrepancy between the nominal mesh and the fine mesh is low, the set-up corresponding to the nominal mesh is applied for all instruments. Regarding the convergence toward a steady state, about 250 iterations are necessary to reach the stabilization of physical quantities defined as goals in the simulation. These quantities are chosen by the user. In the present study, we monitored the

convergence for the following quantities:

- average and maximum velocity for each component in the computational domain,
- min, max and average pressure in the computational domain,
- flow rate and average total pressure through bell exit.

The levels of convergence are below 0.001 Pa for pressures, below 0.004 m/s (0.7%) for velocities and 0.01 l/min (0.1%) for flow rate.

The solver does not provide the monitoring of residuals. Besides, the time step is automatically chosen, in order to fulfill internal stability criteria such as Courant–Friedrichs–Lewy condition while enabling the fastest convergence.